Assessment and Optimization of Cutting Parameters while Turning AISI 52100 Steel

Vishal S Sharma[1,#], Suresh Dhiman[2], Rakesh Sehgal[2] and Surinder Kumar Sharma[3]

1 Department of Industrial Engineering, National Institute of Technology, Jalandhar, Pin 144011 (Pb.), India
2 Department of Mechanical Engineering, National Institute of Technology, Hamirpur, Pin 177001 (HP), India
3 Department of Mechanical Engineering, National Institute of Technology, Kurukshetra, Pin 132118 (Hy.), India
Corresponding Author / E-mail: sharmavs@nitj.ac.in, vishal_sim@yahoo.com, TEL: 91-9872881738, FAX: 91-181-2690320

KEYWORDS: Cutting forces, Tool tip temperature, Surface roughness

This investigation deals with machining AISI 52100 steel using a carbide-coated tool. The machining cutting force and tool tip temperature are measured online while turning using different cutting parameters. The surface roughness is also measured, but off-line after each cut. The obtained data are analyzed and the influence of the cutting parameters on the machining variables is determined in the form of plots. Regression models obtained from the results are tested using additional experimental data.

Manuscript received: September 10, 2007 / Accepted: January 14, 2008

NOMENCLATURE

A = approach angle
B = speed
C = feed
D = depth of cut
F_c = cutting force
F_f = feed force
F_p = passive force
R_a = surface roughness
T_t = tool tip temperature

1. Introduction

The cost of machining amounts to more than 15–20% of the value of manufactured products in industrialized countries. It is therefore imperative to investigate the machinability behavior of different materials by changing the machining parameters to obtain optimal results. The machinability of a material provides an indication of its adaptability to manufacturing by a machining process. Good machinability is defined as an optimal combination of factors such as a low cutting force, good surface finish, low tool tip temperature, and low power consumption.[1,2]

The forces acting on a tool are an important aspect of machining. Knowledge of the cutting forces is needed to estimate the power requirements and ensure that the machine tool elements, tool-holders, and fixtures are adequately rigid and free from vibrations. The cutting forces vary with the tool angle, speed, feed rate, depth of the cut, and approach angle, and accurate measurements of the tool forces are helpful in optimizing the tool design. A scientific analysis of metal cutting also requires knowledge of the tool forces. Dynamometers have been developed that are capable of measuring tool forces with an increasing degree of accuracy. For a semi-orthogonal cutting operation during lathe turning, the force components can be measured in three directions. The force components acting on a tool along with the approach angle are shown in Fig. 1.

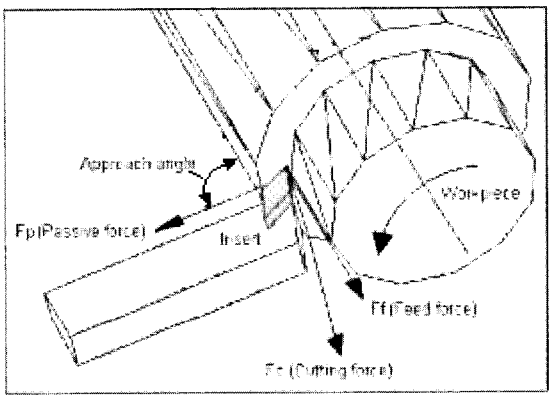

Fig. 1 Cutting forces and approach angle

Measurements of the force and the chip thickness make it possible to explore the stresses obtained under simple orthogonal cutting conditions in which a continuous chip is formed with no built-up edge and the work is sheared in a zone close to the shear plane. For such an analysis, we assume that shear takes place on the shear plane to form the chip. In general, the shear strength of metals and alloys during cutting varies only slightly over a wide range of cutting speeds and feeds provided that the shear plane area remains constant. The force required to form the chip, which is dependent on the shear yield strength of the metal, increases after any alloying or

heat treatment, which raises the yield strength.[3,4]

During metal cutting, the consumed power is largely converted into heat near the cutting edge of the tool. Many of the economic and technical problems of machining are caused directly or indirectly by this heating action. As in all metalworking operations, the energy dissipated in a cutting operation raises the temperature in the cutting zone. Excessive temperatures adversely affect the strength, hardness, and wear resistance of the cutting tool, causing dimensional changes and inducing thermal damage to the machined surface.[5,6]

Haci *et al.*[7] compared the measured and calculated cutting force components and temperature variations generated on the tool tip during turning for different cutting parameters and tools with various tool geometries while machining AISI 1040 steel hardened to HRC 40. The average deviation between the measured and calculated forces was 0.37%. They suggested that the optimum approach and rake angles were 75° and 12°, respectively. For comparison, the main cutting force and tangential force components for different cutting parameters and tool geometries were calculated using the Kienzle approach while the temperature values were calculated based on an orthogonal cutting mechanism.

Chou *et al.*[8] carried out an experimental investigation of cubic boron nitride (CBN) turning of hardened AISI 52100 steel. The performance of the CBN tool on the part surface and the tool flank wear were evaluated. Machining tests showed that low CBN content tools generated better surface finishes and had lower flank wear rates than high CBN counterparts. These tests were performed by changing the speed, feed rate, and depth of cut. The findings of this study suggest that CBN tool performance is not solely dependent on the bulk mechanical properties; instead, the interactions of microstructures between the tool and the transferred layer on the wear land can be important.

Thiele and Melkote[9] conducted an experimental investigation to determine the effects of the tool edge geometry and workpiece hardness on the surface roughness and cutting forces during finish hard turning of AISI 52100 steel. The investigation demonstrated that the cutting edge geometry had a significant effect on the axial and radial cutting force components (or the equivalent thrust force). The effect of the workpiece hardness and edge geometry interaction on the surface roughness was also significant. Increasing the edge hone radius tended to increase the average surface roughness because of the increase in the plowing component compared to the shearing component of deformation.

Guo and Liu[10] designed and conducted a tensile test at elevated temperatures to obtain the mechanical properties of AISI 52100 steel as a function of temperature in both the elastic and plastic regions with large strains. Temperature was the dominant factor for the mechanical properties of this material, while the strain rate effect was secondary. A finite element method (FEM) prediction of the cutting forces and chip geometries agreed with the experimental data to a reasonable degree of accuracy.

Liang *et al.*[11] presented an integrated approach to the simultaneous optimization of machining parameters on mild steel, including machining speed, feed rate, depth of cut, number of passes, tool adjustment interval, and the amount of adjustment. They found that the tool adjustment interval and amount of adjustment depended not only on the amount of material being removed, but also on the cutting speed, feed, and depth of cut.

Chandra *et al.*[12] monitored the cutting force and power consumed in a turning operation for a tool in good condition until it approached its maximum flank wear. They carried out an experimental investigation on mild steel to correlate the rise in cutting force and power expended with the tool wear rate to propose a suitable methodology for estimating tool wear. Tests were carried out on mild steel using a carbide-tipped tool. The results indicated a significant increase in the cutting forces and power as the tool wear progressed in a continuous turning operation. It was possible to the predict tool wear more precisely by continuously monitoring the cutting forces, power, and current for all cutting conditions.

Miller et al.[13] proposed experimental techniques using modern digital infrared imaging that could gather the cutting tool temperature distribution during an orthogonal machining operation. This new process overcame many problems associated with past experimental techniques.

Outeiro *et al.*[14] investigated the effects of the tool geometry, tool coating, and cutting regime parameters on the residual stress distribution of a machined surface and subsurface of AISI 316 L steel using experimental and numerical techniques. They concluded that the residual stresses increased with most of the cutting parameters, including the cutting speed, uncut chip thickness, and tool cutting edge radius. The residual stresses were greater when a coated tool was used, and an increase in the rake angle reduced the residual stresses. The uncut chip thickness had the greatest influence on the residual stresses.

Feng[15] conducted an experimental study of the impact of turning parameters on the surface roughness by using a fractional factorial experimental approach. He determined that the depth of cut did not affect the surface roughness, whereas the feed rate, nose radius, work material, speed, and tool point angle had a significant impact on the observed surface roughness. The most significant interactions were among the work material, point angle, and speed.

Very little has been reported on predicting the machining behavior of AISI 52100 steel under raw conditions (without heat treatment) for different approach angles. Thus, in this study we sought to investigate the effect of the approach angle, speed, feed rate, and depth of cut on the main cutting force components, surface integrity, power consumption, stress, and tool tip temperature. The experimental results were analyzed and evaluated to determine the optimum approach angle.

In this paper, we outline an approach to quantify the specific relationships between the cutting parameters and machining variables. Models are formulated and their performance evaluated with actual experimental data.

2. Experimental Setup and Procedure

AISI 52100 steel was used for this investigation. This material was chosen based on its wide applications in dies and molds, roller and ball bearings, and balls for shot peening, blasting, and barrel cleaning. The chemical composition of AISI 52100 steel was evaluated using a Spark Emission Spectrometer (Baird, USA); the obtained composition is given in Table 1. The hardness of the specimens was tested with a microhardness tester (Akashi MVKH2, Japan) and is also given in Table 1. The machining experiments were carried out on a geared high-precision digital readout lathe using an indexable coated-carbide insert (CCMT090304). These inserts had a multilayer CVD coating and a cobalt-enriched substrate. The CVD coating consisted of a thick, medium-temperature chemical vapor deposition (MTCVD) TiCN (4 μm) for wear resistance and thermally stable Al_2O_3 (8 μm) for crater resistance. The combined top coating and gradient substrate provided extremely good behavior during dry machining. A sketch of the carbide insert used for the tests is shown in Fig. 2.

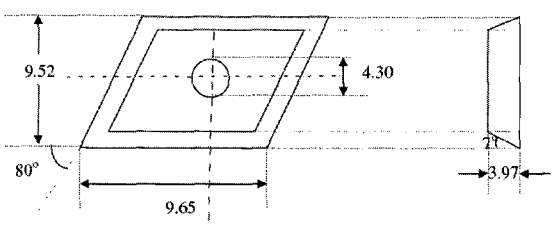

all dimensions in mm

Fig. 2 Sketch of the carbide insert used for machining

The cutting force (F_c), passive force (F_p), feed force (F_f), surface

roughness (R_a), and tool tip temperature (T_t) were measured at different approach angles, speeds, feed rates, and depths of cut. The variation in the cutting parameters used for these tests is given in Appendix I. In total, 29 statistically planned tests were conducted to determine the effect of the cutting parameters on the machining variables. The turning operations were performed using the cutting parameters listed in Table 1.

Table 1 Experimental design

Workpiece material	AISI 52100 steel (%) C = 1.1, Si = 0.3, Mn = 0.6, P = 0.04, S = 0.045, Cr = 1.34, Ni < 0.002, Mo < 0.001	25 HRC
Tool material	carbide-coated insert	CCMT090304
Approach angle	45°, 60°, 90°	
Speed (m/min)	36.6, 126.6, 196	
Feed rate (mm/rev)	0.1, 0.17, 0.27	
Depth of cut (mm)	0.3, 0.9, 1.5	
Rake angle	6°	

A schematic layout of the experimental setup is shown in Fig. 3(a). A three-component turning dynamometer (TeLC DKM 2010, Germany) was used for the tests. Longitudinal turning was performed; the length of the cut for each test was 25 mm. The tool tip temperature was measured with an InGaAs radiation sensor (Impact Electronics Series 300, 24 VDC, 4 – 20 mA). The data acquisition sampling rate was 5 samples/s. The tool tip temperature sensor was mounted in such a manner that it focused a 2-mm-diameter light spot on the tool tip at the back relief face. It was positioned 90 mm from the tool tip inclined at 30° to the axis of the workpiece (refer to Fig. 3(b) and (c)). The turning dynamometer was rigidly held on the tool post so that the cutting forces (F_c, F_f, and F_p) could be measured (refer to Fig. 3(b) and (d)). The force and temperature signals obtained from the dynamometer were transferred to a computer by means of a data acquisition card. These signals were then evaluated using XKM software. A surface roughness tester (SJ-301, Mitotoyo, Japan) was used to measure the surface roughness (R_a) after each turning operation.

2.1 Experimental Design

Tests were performed as described in Appendix I to investigate the influence of the cutting parameters (approach angle, speed, feed, and depth of cut) on the cutting forces (F_c, F_p, and F_f) and surface roughness (R_a). The response surface methodology was employed for to model and analyze the machining parameters during the turning process to obtain the machinability performance of the cutting forces and surface roughness. In the response surface methodology, the quantitative form of the relationship between the desired response and the independent input variables can be represented as

$$Y = F(A, B, C, D) \tag{1}$$

where Y is the desired response and F is the response function. In the analysis, the approximation Y is proposed using a fitted linear model that can be written as

$$Y = a_0 + \sum_{i=1}^{4} a_i X_i \tag{2}$$

where a_0 is constant, a_i represents the coefficients of the linear product terms, and X_i, i = 1,2,3,4 correspond to the studied machining parameters obtained from the following transformation equations:

$$X_1 = \frac{A - A_0}{\Delta A} \tag{3}$$

$$X_2 = \frac{B - B_0}{\Delta B} \tag{4}$$

$$X_3 = \frac{C - C_0}{\Delta C} \tag{5}$$

$$X_4 = \frac{D - D_0}{\Delta D} \tag{6}$$

where X_1, X_2, X_3, and X_4 are the respective coded values of parameters A, B, C, and D; A_0, B_0, C_0, and D_0 are the respective values of A, B, C, and D at zero level; and ΔA, ΔB, ΔC, and ΔD are the intervals of the variation in A, B, C, and D, respectively. The cutting force components (Y_1, Y_2, and Y_3) and surface roughness (Y_4) were analyzed as responses. We used this linear model of F not only to investigate the entire factor space but also to locate the region of the desired target where the responses approach their optimum values.

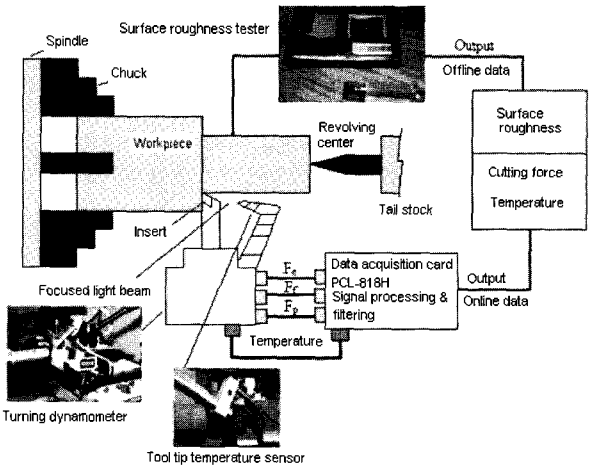

(a)

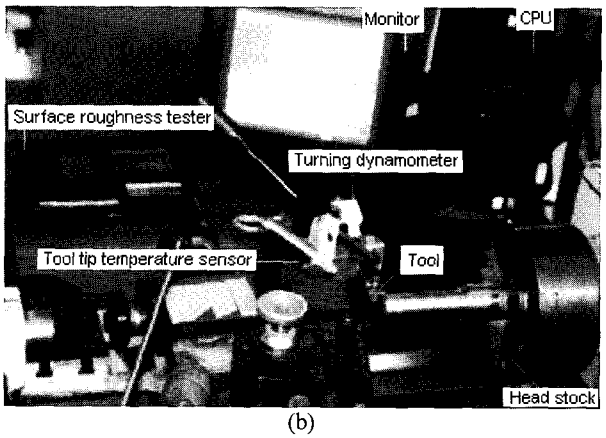

(b)

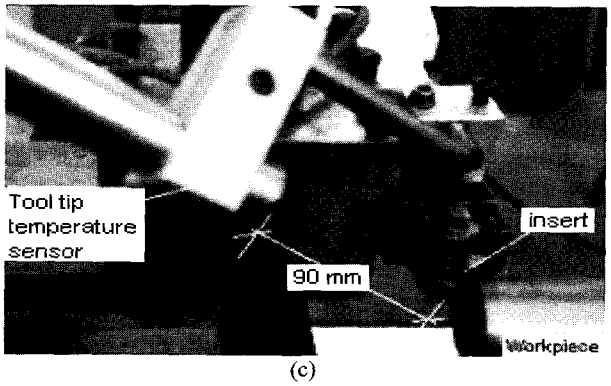

(c)

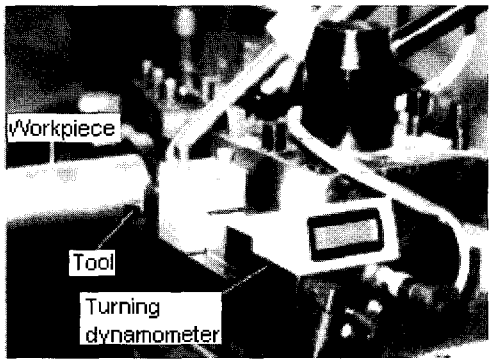

(d)

Fig. 3 Experimental setup. (a) Schematic layout, (b) photograph of the experimental setup, (c) positioning of the tool tip temperature sensor, and (d) turning tool dynamometer

3. Analysis and Discussion

The experimental results of $Y_1(F_c)$, $Y_2(F_p)$, $Y_3(F_f)$, $Y_4(T_t)$, and $Y_5(R_a)$ along with the design matrix are tabulated in the table given in Appendix II. The experimental plan was developed to establish a linear model for Y_1, Y_2, Y_3, and Y_4. Therefore, a test to measure the significance of the regression model on individual model coefficients and a test of the lack of fitting were performed to verify the quality of the fit for the obtained model. An analysis of variances (ANOVA) was applied to summarize these tests. The statistical significance of the fitted linear model for cutting forces and surface roughness was evaluated using the ANOVA F-test. When the values of "Prob > F" in the tables for the terms of the models are less than 0.05 (*i.e.*, $\alpha = 0.05$, or a 95% confidence level), this indicates that the obtained model is statistically significant and the terms in the model have a significant effect on the responses.

3.1 Cutting Force Analysis

Refering to Appendix III, the variance analysis table for the cutting force F_c had a model F value of 967223.55, which implies that the model is significant. Only a 0.01% chance existed that a large model F value would occur due to noise. The values of "Prob > F" were less than 0.0500, indicating that the model terms were significant. In this case, *A*, *B*, *C*, and *D* were significant model terms (*i.e.*, the approach angle, speed, feed, and depth of cut influenced the cutting force). The regression equation obtained for the cutting force in terms of the cutting parameters is

$$F_c = 3.19 + 0.269A - 0.239B + 1338.327C + 294.44D. \quad (7)$$

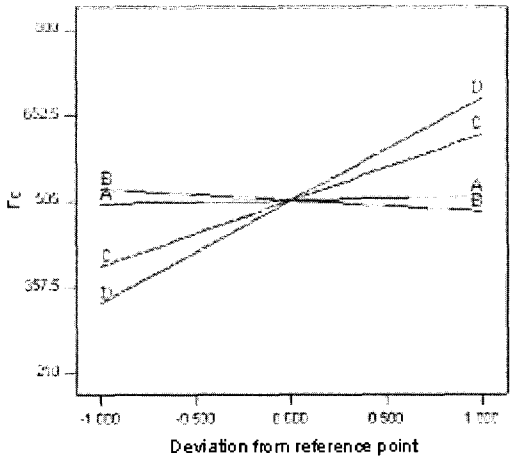

Fig. 4 Effect of the cutting parameters on the cutting force

Figure 4 shows the effects of all the cutting parameters (approach angle, speed, feed, and depth of cut) on the cutting force. The actual factors were *A* (approach angle) = 67.50, *B* (speed) = 116.30, *C* (feed) = 0.19, and *D* (depth of cut) = 0.90. Thus, the feed and depth of cut influenced the cutting force more than the approach angle and speed. The cutting force increased with the feed and depth of cut. The approach angle had almost no contribution to the cutting force, while the cuting force decreased slightly as the speed increased.

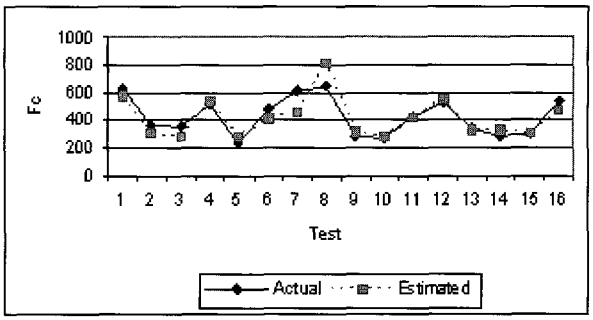

Fig. 5 Comparison of the actual and estimated cutting force

Figure 5 compares the actual and estimated values of the cutting force. The dotted line represents the estimated cutting force while the solid line represents the actual experimental cutting force. The estimated values were obtained using the regression equation. The force was estimated for 16 different cutting parameters (other than those used to construct the model), as shown in Appendix II. Since both the lines are quite close to each other, good agreement was achieved between the estimated and actual experimental values. The average accuracy of the estimated data was 93.26% for this model. Hence, Eq. (7) can be used to estimate the cutting force with a reasonable degree of accuracy.

3.2 Feed Force Analysis

Refering to the Appendix III variance analysis table for feed force, a model F value of 3226.83 implied that the model was significant. Only a 0.01% chance existed that a large model F value would occur due to noise. The values of "Prob > F" were less than 0.0500, indicating that the model terms *A*, *B*, *C*, and *D* were significant. The regression equation obtained for feed force in terms of the cutting parameters is

$$F_f = 123.687 - 1.190A - 0.239B - 143.951C + 128.154D. \quad (8)$$

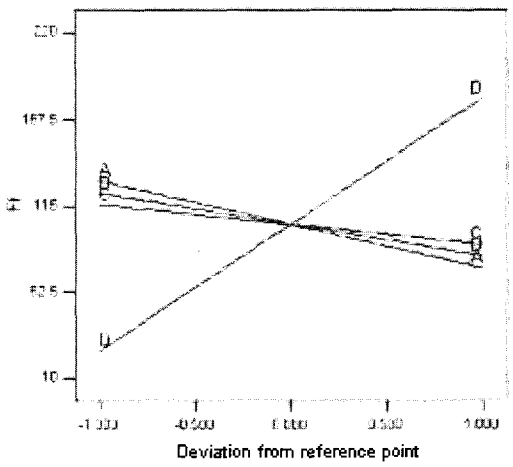

Fig. 6 Effect of the cutting parameters on the feed force

Figure 6 shows the effect of the various cutting parameters on the feed force. The feed force decreased as the approach angle, speed, and feed increased while the feed force increased with the depth of cut. The actual and estimated feed force values are compared in Fig. 7 in the same way that the cutting force values were compared in Fig. 5. Good agreement was achieved between the estimated and

actual experimental values; the average accuracy of the predications of this model was 99%.

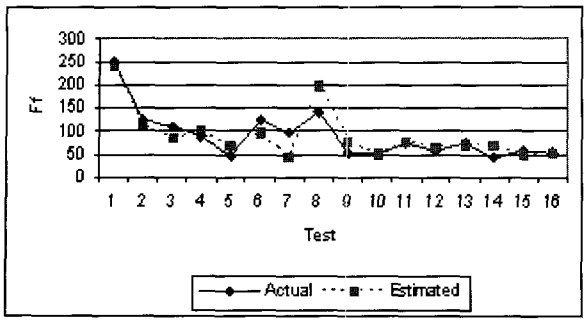

Fig. 7 Comparison of the actual and estimated feed force

3.3 Passive Force Analysis

The same analysis was performed for the passive force and is summarized in the passive force variance table in Apppendix III. A model F value of 40125.97 implied that the model was significant and only a 0.01% chance existed that a large model F value would occur due to noise. The values of "Prob > F" were less than 0.0500. The regression equation obtained for the passive force in terms of the cutting parameter is

$$F_p = 294.305 - 2.038A + 0.069B + 889.355C + 62.580D. \quad (9)$$

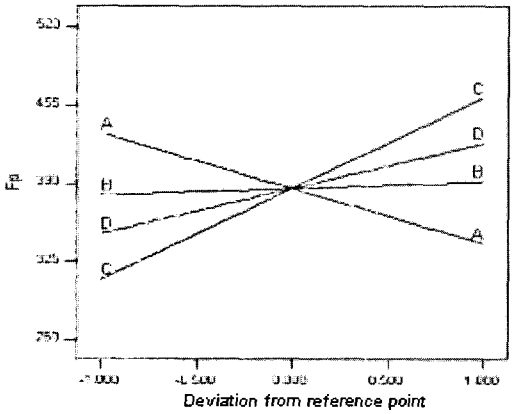

Fig. 8 Effect of the cutting parameters on the passive force

Figure 8 shows the effect of various cutting parameters on the passive force. The passive force decreased with increasing approach angle and increased with increasing feed rate and depth of cut. The speed had little effect on the passive force. The actual and estimated values are compared in Fig. 9 in the same manner as before. The average accuracy of the predications was 97%.

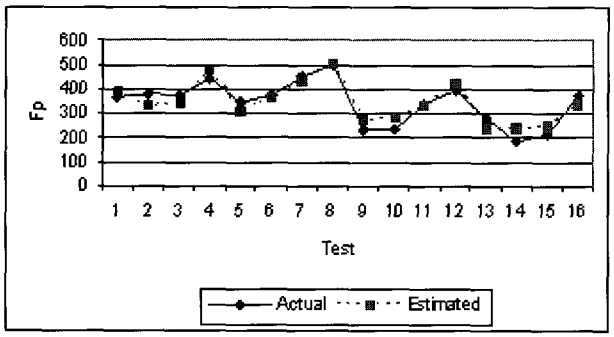

Fig. 9 Comparison of the actual and estimated passive force

3.4 Tool Tip Temperature Analysis

A model F value of 13597.40 (see Appendix III) implied that the model was significant. Only a 0.04% chance existed that a model F value this large would occur due to noise. The values of "Prob > F" were less than 0.0500. The regression equation obtained for the tool tip temperature in terms of the cutting parameters is

$$T_t = 482.637 - 1.031A + 0.110B - 160.118C + 22.650D. \quad (10)$$

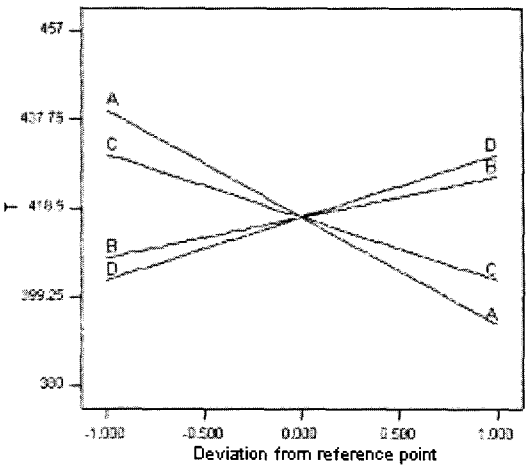

Fig. 10 Effect of the cutting parameters on the tool tip temperature

Figure 10 shows the effect of the various cutting parameters. The tool tip temperature decreased with increasing appraoch angle and feed, and increased with increasing speed and depth of cut. The comparison between the actual and estimated values of the tool tip temperature, shown in Fig. 11, indicated that the average prediction accuracy for this model was 99%.

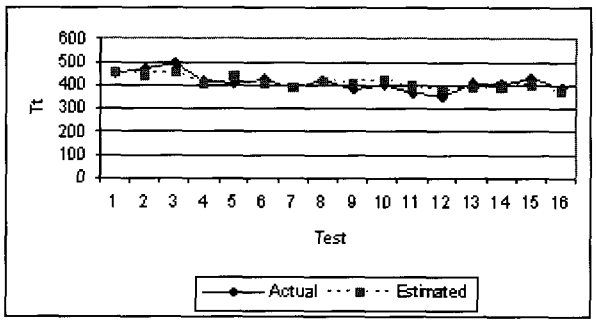

Fig. 11 Comparison of the actual and estimated tool tip temperature

3.5 Surface Roughness Analysis

A model F value of 676.42 (see Appendix III) implied that the model was significant. Only a 0.01% chance existed that a model F value this large would occur due to noise. The values of "Prob > F" were less than 0.0500. The regression equation obtained for the surface roughness in terms of the cutting parameters is

$$R_a = 3.184 - 0.072A + 4.19350 \times 10^{-3}B + 116.992C - 1.75D \quad (11)$$

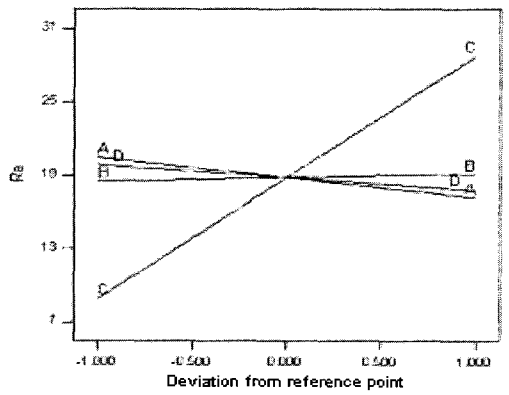

Fig. 12 Effect of the cutting parameters on the surface roughness

Figure 12 shows the effect of the various cutting parameters. The surface roughness increased with the feed rate. The feed rate had the most influence of all the cutting parameters. The speed had little

effect, and the surface roughness decreased slightly with increasing approach angle and depth of cut. The actual and estimated values are compared in Fig. 13. The average prediction accuracy for this model was 99.5%.

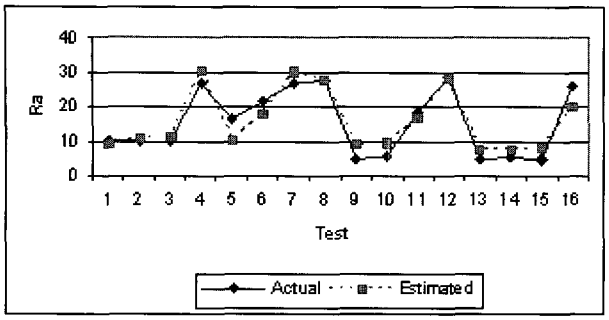

Fig. 13 Comparison of the actual and estimated surface roughness

4. Optimization

The objective of the optimization was to find cutting parameters within an approach angle range of 45° to 90°, speed range of 36.6 to 196 m/min, feed range of 0.1 to 0.27 mm/rev, and depth of cut range of 0.3 to 1.5 mm such that the cutting force components F_c, F_p, and F_f, tool tip temperature T_t, and surface roughness R_a were minimized. The optimum results are given in Appendix IV. The best result consisted of an approach angle of 89.9°, a speed of 50.79 m/min, a feed rate of 0.10 mm/rev, and a depth of cut of 0.30 mm. This gave a cutting force F_c of 237.45 N, a feed force F_f of 28.44 N, a passive force F_p of 222.07 N, a tool tip temperature T_t of 386.19°C, and a surface roughness R_a of 8.06 μm, corresponding to a desirability of 0.951.

5. Conclusions

We measured machining variables such as cutting force, tool tip temperature, and surface roughness while turning AISI 52100 steel on a lathe. The effects of the cutting parameters such as approach angle, speed, feed rate, and depth of cut on the machining variables were evaluated. The data obtained from experiments were used to construct regression models using ANOVA. The models were then tested with additional experimental data and the results were compiled. The following conclusions can be drawn.

1. All the regression models derived in the study performed well.
2. The cutting force increased with the feed rate and depth of cut. The approach angle had little effect of the cutting force, and increasing the speed caused the cutting force to decrease slightly.
3. The feed force increased with increasing depth of cut and decreased with increasing approach angle, speed, and feed rate.
4. The passive force dcreased with increasing approach angle and decreased with increasing feed rate and depth of cut. The speed had little effect on the passive force.
5. The tool tip temperature decreased with increasing appraoch angle and feed rate, and increased with increasing speed and depth of cut.
6. The surface roughnesss increased with increasing feed rate. The speed had little effect on the surface roughness, and the surface roughness decreased slightly with increasing approach angle and depth of cut.

Increasing the approach angle decreased the cutting force, feed force, passive force, tool tip temperature, and surface roughness. Increasing the speed increased the passive force, tool tip temperature, and surface roughness, and decreased the cutting force and feed force. Increasing the feed rate increased the cutting force, passive force, and surface roughness and decreased the tool tip temperature and feed force. Increasing the depth of cut increased the cutting force, passive force, feed force, and tool tip temperature, and decreased the surface roughness.

REFERENCES

1. Noordin, M. Y., Venkatesh, V. C., Sharif, S., Elting, S. and Abdullah, A., "Application of response surface methodology in describing the performance of coated carbide tools when turning AISI 1045 steel," Journal of Material Processing Technology, Vol. 145, No. 1, pp. 46-58, 2004.
2. Heo, S. J., "Machining Characteristics of Cemented Carbides in Micro Cutting within SEM," International Journal of Precision Engineering and Manufacturing, Vol. 5, No. 3, pp. 35-42, 2004.
3. Trent, E. M. and Wright, P. K., "Metal Cutting," Butterworth–Heinemann, pp. 9-95, 2000.
4. Jung, J. W., Ko, S. H., Jeong, Y. H., Min, B. K. and Lee, S. J., "Estimation of Material Removal Volume of a Micro-EDM Drilled Hole Using Discharge Pulse Monitoring," International Journal of Precision Engineering and Manufacturing, Vol. 8, No. 4, pp. 45-49, 2007.
5. Kalpakjian, S., "Manufacturing Engineering and Technology," Addison–Wesley Publishing Company, pp. 589-635, 1989.
6. Kim, K. W. and Ahn, T. K., "Force Prediction and Stress Analysis of a Twist Drill from Tool Geometry and Cutting Conditions," International Journal of Precision Engineering and Manufacturing, Vol. 6, No. 1, pp. 65-72, 2005.
7. Haci, S., Faruk, U. and Yaldiz, S., "Investigation of the effect of rake angle and approaching angle on main cutting force and tool tip temperature," International Journal of Machine Tools and Manufacture, Vol. 46, Issue 2, pp. 132-141, 2006.
8. Chou, Y. K., Evans, C. J. and Barash, M. M., "Experimental investigation on cubic boron nitride turning of hardened AISI 52100 steel," Journal of Material Processing Technology, Vol. 134, Issue 1, pp. 1-9, 2003.
9. Thiele, J. D. and Melkote, S. N., "Effect of cutting edge geometry and workpiece hardness on surface generation in the finish hard turning of AISI 52100 steel," Journal of Material Processing Technology, Vol. 94, Issues 2-3, pp. 216-226, 1999.
10. Guo, Y. B. and Liu, C. R., "Mechanical properties of hardened AISI 52100 steel in hard machining processes," Journal of Manufacturing Science and Engineering, Vol. 124, Issue 1, pp. 1-9, 2002.
11. Liang, M., Mgwalu, M. and Zuo, M., "Integration of cutting parameters selection and tool adjustment decisions for multipass turning," International Journal of Advanced Manufacturing Technology, Vol. 17, No. 12, pp. 861-869, 2001.
12. Chandra, M. R. G, Komaraiah, M., Kamala, V., Prashanth, J. P. and Bala, K. K., "Condition monitoring of cutting force and power in a turning operation with tool wear," Sixteenth National Convention of Mechanical Engineers and National Seminar on Future Trends in Mechanical Engineering, pp. 546-551, 2000.
13. Miller, M. R., Mulholland, G. and Anderson, C., "Experimental cutting tool temperature distributions," Journal of Manufacturing Science and Engineering, Vol. 125, Issue 4, pp. 667-673, 2003.
14. Outeiro, J. C., Umbrello, D. and Saoubi, R. M., "Experimental and numerical modeling of the residual stresses induced in orthogonal cutting of AISI 316 L steel," International Journal of Machine Tool and Manufacturing, Vol. 46, Issue 14, pp. 1786-

1794, 2006.

15. Feng, C. X., "An experimental study of the impact of turning parameters on surface roughness," Proceedings of the Industrial Engineering Research Conference, No. 2036, pp. 1-7, 2001.

APPENDIX I: Experimental Values

A: Approach angle (°)	*B*: Speed (m/min)	*C*: Feed rate (mm/rev)	*D*: Depth of cut (mm)	F_c (N)	F_f (N)	F_p (N)	T_t (°C)	R_a (μm)
60	126.6	0.17	0.9	481.4849	112.556	388.4163	427.7729	17.509
60	126.6	0.27	1.5	791.9859	176.324	514.8833	425.3699	28.193
60	126.6	0.17	0.9	480.158	113.556	389.951	429.357	19.753
45	126.6	0.1	0.9	383.749	141.323	356.773	454.418	10.3452
60	196	0.1	0.9	371.143	105.917	331.031	446.602	9.5672
60	126.6	0.17	0.9	482.598	111.258	385.987	428.753	20.156
45	196	0.17	0.9	460.7789	114.65	423.8743	450.8569	18.831
90	126.6	0.17	0.3	312.9209	11.2	289.6683	383.2829	16.459
45	126.6	0.27	0.9	611.2719	116.996	507.9353	427.2299	30.293
60	36.6	0.17	1.5	679.7489	212.234	419.6643	431.4629	16.1062
60	36.6	0.27	0.9	636.9219	119.846	471.0353	401.8799	28.8902
90	196	0.17	0.9	472.9289	58.4	332.0743	404.5069	15.681
45	126.6	0.17	0.3	300.7709	53.228	381.4683	429.6329	19.609
60	126.6	0.17	0.9	481.985	112.963	389.697	426.773	17.509
60	126.6	0.27	0.3	438.6579	20.168	439.7873	398.1899	30.293
60	196	0.27	0.9	598.6659	81.59	482.1933	419.4139	29.515
90	126.6	0.27	0.9	623.4219	60.746	416.1353	380.8799	27.143
60	126.6	0.17	0.9	481.796	111.369	385.694	428.863	17.509
90	126.6	0.1	0.9	395.899	85.073	264.973	408.068	7.1952
60	36.6	0.17	0.3	326.4209	56.078	344.5683	404.2829	18.2062
60	196	0.17	1.5	641.4929	173.978	430.8223	448.9969	16.731
45	36.6	0.17	0.9	499.0349	152.906	412.7163	433.3229	18.2062
60	126.6	0.1	0.3	211.135	44.495	288.625	425.378	10.3452
60	126.6	0.1	1.5	564.463	200.651	363.721	452.558	8.2452
60	196	0.17	0.3	288.1649	17.822	355.7263	421.8169	18.831
90	36.6	0.17	0.9	511.1849	96.656	320.9163	386.9729	15.0562
90	126.6	0.17	1.5	666.2489	153.134	364.7643	410.4629	14.359
60	36.6	0.1	0.9	409.399	144.173	319.873	429.068	8.9424
45	126.6	0.17	1.5	654.0989	209.384	456.5643	456.8129	17.509

APPENDIX II: Actual and Estimated Values

Actual values

A: Approach angle (°)	*B*: Speed (m/min)	*C*: Feed rate (mm/rev)	*D*: Depth of cut (mm)	F_c (N)	F_f (N)	F_p (N)	T_t (°C)	R_a (μm)
45	36.6	0.1	1.5	630	250	364	450	10.21
45	81.7	0.1	0.6	359	123	382	470	9.88
45	196	0.1	0.6	348	109	373	493	9.93
45	36.6	0.27	0.6	513	90	448	416	27.04
60	196	0.1	0.6	237	46	343	409	16.25
60	36.6	0.171	0.6	477	122	376	421	21.6
60	36.6	0.27	0.3	610	95	455	390	26.8
60	36.6	0.27	1.5	652	142	499	422	27.8
75	81.7	0.1	0.6	282	52	232	380	4.94
75	196	0.1	0.6	265	49	235	405	5.58
75	36.6	0.171	0.6	423	74	336	370	18.58
75	36.6	0.27	0.6	532	57	395	354	28.78
90	36.6	0.1	0.6	336	75	284	407	4.81
90	51.5	0.1	0.6	288	42	185	400	5.28
90	126.6	0.1	0.6	306	55	214	431	4.76
90	36.6	0.21	0.6	547	54	373	391	25.87

Estimated values

A: Approach Angle (°)	*B*: Speed (m/min)	*C*: Feed rate (mm/rev)	*D*: Depth of Cut (mm)	F_c (N)	F_f (N)	F_p (N)	T_t (°C)	R_a (μm)
45	36.6	0.1	1.5	582.0389	239.1971	387.9184	458.2242	9.1567
45	81.7	0.1	0.6	306.2203	113.0641	334.7475	442.807	10.9208
45	196	0.1	0.6	278.7917	85.7087	342.7336	455.3972	11.4001
45	36.6	0.27	0.6	544.5586	99.386	482.7869	410.6191	30.6204
60	196	0.1	0.6	282.8374	67.8528	312.1504	439.928	10.3148
60	36.6	0.171	0.6	416.1098	95.7814	364.1575	411.0016	17.9528
60	36.6	0.27	0.3	460.2723	43.0838	433.4297	388.3549	30.0601
60	36.6	0.27	1.5	813.6003	196.8694	508.5257	415.5349	27.9601
75	81.7	0.1	0.6	314.3116	77.3524	273.5811	411.8686	8.7502
75	196	0.1	0.6	286.883	49.997	281.5672	424.4588	9.2295
75	36.6	0.171	0.6	420.1555	77.9256	333.5743	395.5324	16.8675
75	36.6	0.27	0.6	552.6499	63.6743	421.6205	379.6807	28.4498
90	36.6	0.1	0.6	329.1799	70.2903	239.8468	391.4316	7.4757
90	51.5	0.1	0.6	325.6043	66.7243	240.8879	393.0729	7.5382
90	126.6	0.1	0.6	307.5826	48.7506	246.135	401.3451	7.8531
90	36.6	0.21	0.6	476.3959	54.4556	337.676	373.8186	20.3449

APPENDIX III: ANOVA Tables

Variance analysis table for cutting force

Source	Sum of squares	df	Mean square	F value	p-value Prob > F	
Model	537366.2	4	134341.6	967223.5	<0.0001	significant
A: Approach angle	470.6938	1	470.6938	3388.87	<0.0001	
B: Speed	4432.251	1	4432.251	31911.03	<0.0001	
C: Feed rate	158121.3	1	158121.3	1138431	<0.0001	
D: Depth of cut	374522	1	374522	2696459	<0.0001	
Residual	3.333456	24	0.138894			
Cor Total	537369.6	28				

Variance analysis table for feed force

Source	Sum of squares	df	Mean square	F value	p-value Prob > F	
Model	86372.95	4	21593.24	3226.832	<0.0001	significant
A: Approach angle	9168.84	1	9168.84	1370.165	<0.0001	
B: Speed	4408.705	1	4408.705	658.8242	<0.0001	
C: Feed rate	1829.365	1	1829.365	273.375	<0.0001	
D: Depth of cut	70950.09	1	70950.09	10602.58	<0.0001	
Residual	160.6027	24	6.691777			
Cor Total	86533.56	28				

Analysis of variance table for passive force (Fp)

Source	Sum of squares	df	Mean square	F value	p-value Prob > F	
Model	114411.5	4	28602.88	40125.97	<0.0001	significant
A: Approach angle	26897.88	1	26897.88	37734.09	<0.0001	
B: Speed	375.7464	1	375.7464	527.1214	<0.0001	
C: Feed rate	69825.91	1	69825.91	97956.32	<0.0001	
D: Depth of cut	16918.23	1	16918.23	23733.99	<0.0001	
Residual	17.10785	24	0.712827			
Cor Total	114428.6	28				

Analysis of variance table for tool tip temperature (Tt)

Source	Sum of squares	df	Mean square	F value	p-value Prob > F	
Model	12237.24	4	3059.309	13597.4	<0.0001	significant
A: Approach angle	6881.581	1	6881.581	30585.86	<0.0001	
B: Speed	933.8578	1	933.8578	4150.622	<0.0001	
C: Feed rate	2263.332	1	2263.332	10059.6	<0.0001	
D: Depth of cut	2216.257	1	2216.257	9850.372	<0.0001	
Residual	5.399813	24	0.224992			
Cor Total	12242.64	28				

Analysis of variance table for Surface roughness (Ra)

Source	Sum of squares	df	Mean square	F value	p-value Prob > F	
Model	1258.752	4	314.6881	676.4231	<0.0001	significant
A: Approach angle	33.87435	1	33.87435	72.81301	<0.0001	
B: Speed	1.353559	1	1.353559	2.909479	0.1010	
C: Feed rate	1208.324	1	1208.324	2597.297	<0.0001	
D: Depth of cut	13.23	1	13.23	28.43793	<0.0001	
Residual	11.16537	24	0.465224			
Cor Total	1269.918	28				

APPENDIX IV: Optimized Results

A: Approach angle (°)	*B*: Speed (m/min)	*C*: Feed rate (mm/rev)	*D*: Depth of cut (mm)	F_c (N)	F_f (N)	F_p (N)	T_t (°C)	R_a (μm)	Desirability
89.99989	50.79525	0.100008	0.300001	237.4534	28.44579	222.0728	386.1992	8.061241	0.951819
89.98998	44.44562	0.100002	0.300001	238.9657	29.97816	221.6437	385.511	8.034574	0.95178
89.99951	56.52076	0.100048	0.300002	236.1327	27.07047	222.509	386.8239	8.089906	0.951754
89.9999	52.5851	0.100001	0.300242	237.0847	28.04945	222.2062	386.403	8.067431	0.951753
89.99912	62.19625	0.100001	0.300006	234.7088	25.71978	222.8647	387.457	8.108236	0.951737
89.99989	61.54673	0.100026	0.300001	234.8971	25.87006	222.8398	387.3806	8.108407	0.951728
89.99998	71.52762	0.100032	0.300008	232.5121	23.48128	223.5428	388.479	8.150946	0.951565
89.99963	78.6217	0.100001	0.300002	230.7667	21.78761	224.0113	389.2656	8.177115	0.951429
89.99877	36.60016	0.100394	0.300002	241.3762	31.78896	221.4266	384.575	8.046946	0.951425
89.95673	76.72876	0.100014	0.300003	231.2272	22.29001	223.9782	389.0993	8.173803	0.951267